

Radion Phenomenology with 3 and 4 Generations

Mariana Frank^{*,1}, Beste Korutlu^{†,1} and Manuel Toharia^{‡1}

¹*Department of Physics, Concordia University*

7141 Sherbrooke St. West, Montreal

Quebec, CANADA H4B 1R6

(Dated: February 18, 2022)

Abstract

We study radion phenomenology in an warped extra-dimension scenario with Standard Model fields in the bulk, with and without an additional fourth family of fermions. The radion couplings with the fermions will be generically misaligned with respect to the Standard Model fermion mass matrices, therefore producing some amount of flavor violating couplings and potentially influencing production and decay rates of the radion. Simple analytic expressions for the radion-fermion couplings are obtained with three or four families. We also update and analyze the current experimental limits on radion couplings and on the model parameters, again with both three and four families scenarios. We finally present the modified decay branching ratios of the radion with an emphasis on the new channels involving flavor diagonal and flavor violating decays into fourth generation quarks and leptons.

PACS numbers: 12.60.-i, 11.10.Kk, 14.80.-j

* mfrank@alcor.concordia.ca

† bkorutlu@physics.concordia.ca

‡ mtoharia@physics.concordia.ca

I. INTRODUCTION

Warped extra dimensional models have been introduced to explain the origin of the discrepancy between Planck scale and the electroweak scale [1]. In the original scenario, two branes are introduced, one with an energy scale set at the Planck scale, the other at the TeV scale, and with the Standard Model (SM) fields localized on the TeV brane and gravity allowed to propagate in the bulk. However, in this scenario, higher dimensional operators of the IR fields in the 4-dimensional effective theory are only suppressed by TeV scales, leading to large flavor violation and rapid proton decay.

Allowing SM fermions and gauge fields to propagate in the bulk effectively suppresses such operators and can also be used to explain the fermion mass hierarchy by fermion localization [2, 3]. The drawback is that, in minimal models, excitations of the bulk fields are subjected to tight bounds from precision electroweak tests [4] and from flavor physics [5], and constrained to be heavier than a few TeV, making it very hard to produce and observe heavy resonances of these masses at the LHC.

One hope to observe new states from these scenarios might be the radion graviscalar and its associated phenomenology. The radion is a scalar field associated with fluctuations in the size of the extra dimension, and is a novel feature of warped extra dimensional models [1]. The mass of the radion depends on the mechanism that stabilizes the size of the extra dimension. In a simple model with a bulk scalar which generates a vacuum expectation value (VEV), the radion field emerges as a pseudo-Goldstone boson associated with breaking of translation symmetry [6]. Generically, the radion may be the lightest new state in an RS-type setup, with its mass suppressed with respect to KK fields by a volume factor of ~ 40 , at least in the small backreaction limit [7]. This might put its mass between a few tens to hundreds of GeV, with couplings allowing it to have escaped detection at LEP, and consistent with precision EW data CHL. In general, the radion couplings are similar to Higgs couplings in that they are proportional to the mass of the particles it couples with. Moreover the radion field can mix with the Higgs boson after EWSB, which involves another parameter, the coefficient of the curvature-scalar term [8]. Radion phenomenology with and without Higgs-radion mixing has been discussed in several papers [9, 10]. More recently it has been shown that a tree-level misalignment between the flavor structure of the Yukawa couplings of the radion and the fermion mass matrix will appear when the fermion bulk parameters are not all degenerate [11]. The mechanism responsible for these flavor-changing neutral currents (FCNC's) is different than the one producing Higgs mediated FCNC's in these same models [12, 13].

New data seems to indicate some inconsistencies with the SM predictions as pertaining to the the third generation [14]. The simplest explanation is that the Cabibbo-Kobayashi-

Maskawa (CKM) mixing matrix deviates from the standard, three-generation form [15]. A simple extension of the SM to four generations, SM4, (adding a new family of quarks and leptons, mirroring the existing ones) alleviates the problem, and may offer resolutions to some other outstanding problems in the SM [16].

Recently, we have shown that, if the fourth generation is incorporated into warped space models, the flavor-changing couplings of the Higgs boson can be enhanced, and both the production and decays of the Higgs bosons and the decay pattern of the heavy quarks and leptons is altered significantly with respect to the patterns expected in SM4, thus giving rise to distinguishing signals at the colliders [17]. It is thus expected that in a warped scenario with extra generations (seen as a natural extension of the warped space model), the flavor-changing couplings of the radion will also yield characteristic signals at colliders.

There are several reasons to perform a separate study for the radion flavor-changing interactions. A priori, we expect the radion phenomenology to be very different from the Higgs boson in four generations. As will be explained later in the text, the production cross section for the Higgs bosons in 4 generations is enhanced by a factor of about 10, while the production cross section for the radion will remain essentially unchanged by the presence of an extra family. Also, contrary to the Higgs phenomenology in these models [17], exotic flavor violating decays of heavy quarks into radions $Q \rightarrow \phi q$ should be highly suppressed with the new flavor violating couplings of the radion. These will become important in radion decays into quarks $\phi \rightarrow qq, qq'$ as well as into leptons $\phi \rightarrow \tau'\tau$ and $\phi \rightarrow \nu_4\nu_\tau$. Very recent data from ATLAS [19] and CMS [20] experiments at the LHC indicate that a Higgs boson in a scenario with four generations must be very heavy. These measurements do not affect the radion mass directly, but will set limits on the combined radion mass–interaction scale parameter space. While we stated that the phenomenology with three and four generations is quite similar, there are (new) FCNC effects of fourth generation quarks and leptons interacting with the radion.

Our paper is organized as follows. In the next section (Sec. II), we briefly review the warped model with fermions in the bulk, concentrating in particular on the misalignment between the fermion masses and radion-fermion Yukawa couplings. We describe in more detail the flavor structure with four families in Sec III, and proceed to evaluate the radion FCNC couplings, presenting both analytical and numerical results in Sec. IV. We discuss phenomenological constraints in Sec. V and branching ratios in Sec. VI. We summarize and conclude in Sec. VII. Some details of our calculations are left to the Appendix.

II. THE MODEL

The radion graviscalar can be thought of as a scalar component of the 5D gravitational perturbations, and basically it tracks fluctuations of size of the extra-dimension (i.e. its “radius”). The AdS metric including the scalar perturbation F corresponding to the effect of the radion is given in the RS coordinate system by [21]

$$ds^2 = e^{-2(A+F)}\eta_{\mu\nu} - (1 + 2F)^2 dy^2 = \left(\frac{R}{z}\right)^2 (e^{-2F}\eta_{\mu\nu}dx^\mu dx^\nu - (1 + 2F)^2 dz^2), \quad (1)$$

where $A(y) = ky$. Note that the perturbed metric is no longer conformally flat, even in z coordinates. At linear order in the fluctuation, F , the metric perturbation is given by

$$\delta(ds^2) \approx -2F (e^{-2A}\eta_{\mu\nu}dx^\mu dx^\nu + 2 dy^2) = -2F \left(\frac{R}{z}\right)^2 (\eta_{\mu\nu}dx^\mu dx^\nu + 2dz^2). \quad (2)$$

In the absence of a stabilizing mechanism, the radion is precisely massless, however it was shown that the addition of a bulk scalar field with a vacuum expectation value (VEV) leads to an effective potential for the radion after taking into account the back-reaction of the geometry due to the scalar field VEV profile [7]. In the analysis that follows, we assume that this back-reaction is small, and does not have a large effect on the 5D profile of the radion.

The relation between the canonically normalized 4D radion field $\phi(x)$ and the metric perturbation $F(z, x)$ is given by

$$F(z, x) = \frac{1}{\sqrt{6}} \frac{R^2}{R'} \left(\frac{z}{R}\right)^2 \phi(x) = \frac{\phi(x)}{\Lambda_\phi} \left(\frac{z}{R'}\right)^2, \quad (3)$$

with $\Lambda_\phi \equiv \frac{\sqrt{6}}{R'}$ the radion interaction scale.

The 5D interaction terms between the radion and the bulk SM fermion fields are given by the action:

$$S_{\text{fermion}} = \int d^4x dz \sqrt{g} \left[\frac{i}{2} (\bar{\mathcal{Q}}_i \Gamma^A \mathcal{D}_A \mathcal{Q}_i - \mathcal{D}_A \bar{\mathcal{Q}}_i \Gamma^A \mathcal{Q}_i) + \frac{c_{q_i}}{R} \bar{\mathcal{Q}}_i \mathcal{Q}_i - \frac{c_{u_i}}{R} \bar{\mathcal{U}}_i \mathcal{U}_i - \frac{c_{d_i}}{R} \bar{\mathcal{D}}_i \mathcal{D}_i + \left(Y_{ij} \sqrt{R} \bar{\mathcal{Q}}_i \mathcal{H} \mathcal{U}_j + h.c. \right) \right], \quad (4)$$

where $\frac{c_{q_i}}{R}$, $\frac{c_{u_i}}{R}$ and $\frac{c_{d_i}}{R}$ are the 5D fermion masses, and we choose to work in the basis where these are diagonal in 5D flavor space. The Higgs boson in the bulk acquires a VEV $v(z)$ localized towards the IR brane thus solving the Planck-weak hierarchy problem.

One can express the 5D fermions in two component notation,

$$\mathcal{Q}_i = \begin{pmatrix} \mathcal{Q}_L^i \\ \bar{\mathcal{Q}}_R^i \end{pmatrix}, \quad \mathcal{U}_i = \begin{pmatrix} \mathcal{U}_L^i \\ \bar{\mathcal{U}}_R^i \end{pmatrix}, \quad \mathcal{D}_i = \begin{pmatrix} \mathcal{D}_L^i \\ \bar{\mathcal{D}}_R^i \end{pmatrix}, \quad (5)$$

and perform a “mixed” KK decomposition as

$$\begin{aligned}
\mathcal{Q}_L^i(x, z) &= \sum_j Q_L^{ij}(z) q_L^j(x), & \bar{\mathcal{Q}}_R^i(x, z) &= \sum_j Q_R^{ij}(z) \bar{u}_R^j(x), \\
\mathcal{U}_L^i(x, z) &= \sum_j U_L^{ij}(z) q_L^j(x), & \bar{\mathcal{U}}_R^i(x, z) &= \sum_j U_R^{ij}(z) \bar{u}_R^j(x), \\
\mathcal{D}_L^i(x, z) &= \sum_j D_L^{ij}(z) q_L^j(x), & \bar{\mathcal{D}}_R^i(x, z) &= \sum_j D_R^{ij}(z) \bar{d}_R^j(x).
\end{aligned} \tag{6}$$

Here $q_L^j(x)$, $u_R^j(x)$ and $d_R^j(x)$ are the 4D fermions and $Q_{L,R}^{ij}(z)$, $U_{L,R}^{ij}(z)$ and $D_{L,R}^{ij}(z)$ are the corresponding profiles along the extra dimension. The fields $q_L^i(x)$, $u_R^j(x)$ and $d_R^j(x)$ satisfy the Dirac equation

$$-i\bar{\sigma}^\mu \partial_\mu q_L^i + m_{ij}^u \bar{u}_R^j = 0, \tag{7}$$

$$-i\sigma^\mu \partial_\mu q_L^i + m_{ij}^d \bar{d}_R^j = 0. \tag{8}$$

The 4D SM fermion mass matrix m_{ij} is the eigenvalue which emerges from the solution of the coupled bulk equations of motion, and is not necessarily diagonal in flavor space. The couplings between the radion and SM fermions can be obtained by inserting the perturbed metric and the 5D fermion KK decompositions of Eq. (6) into the action of Eq. (4). We proceed by using a perturbative approach in treating the 4D fermion masses m_{ij} as small expansion parameters and keeping only first order terms. A 5D bulk Higgs is considered and its field perturbation contains itself some radion degree of freedom. Including all the contributions, the radion coupling to fermions can be expressed finally as

$$-\frac{\phi(x)}{\Lambda_\phi} (q_L^i u_R^j + \bar{q}_L^i \bar{u}_R^j) m_{ij}^u [\mathcal{I}(c_{q_i}) + \mathcal{I}(c_{u_j})] + (u \rightarrow d), \tag{9}$$

with the definition

$$\mathcal{I}(c) = \left[\frac{(\frac{1}{2} - c)}{1 - (R/R')^{1-2c}} + c \right] \approx \begin{cases} c & (c > 1/2) \\ \frac{1}{2} & (c < 1/2) \end{cases}. \tag{10}$$

This result from [11] is consistent with the original calculation obtained for the case of a brane Higgs and a single family of fermions in [10].

Non-universalities in the term $[\mathcal{I}(c_{q_i}) + \mathcal{I}(c_{u_j})]$ will lead to a misalignment between the Radion couplings and the fermion mass matrix. After diagonalizing the fermion mass matrix, flavor violating couplings of the u-type quarks and radion will be generated, with straightforward extensions to the down quark and lepton sectors. We study these in Sec. IV, after describing the flavor structure of the model with four generations.

III. FLAVOR STRUCTURE WITH FOUR FAMILIES

Warped scenarios have been used before to study an extension of the SM with four generations [23]. Our emphasis is here on flavor-changing interactions between the radion and the fermions. The fermion mass matrices are

$$\mathbf{m}_u = F_Q Y_u F_u, \quad (11)$$

$$\mathbf{m}_d = F_Q Y_d F_d, \quad (12)$$

where F_Q , F_u and F_d are 4×4 diagonal matrices whose entries are given by the values at the IR brane of the corresponding zero-mode wave functions:

$$F_Q = \text{Diag}(f_{Q_1}, f_{Q_2}, f_{Q_3}, f_{Q_4}), \quad F_u = \text{Diag}(f_{u_1}, f_{u_2}, f_{u_3}, f_{u_4}), \quad F_d = \text{Diag}(f_{d_1}, f_{d_2}, f_{d_3}, f_{d_4}) \quad (13)$$

where $f(c)$ is given by

$$f(c) = \sqrt{\frac{1-2c}{1-(R/R')^{1-2c}}} \quad (14)$$

The matrices Y_u and Y_d are the 5-dimensional Yukawa couplings, i.e. general 4×4 complex matrices. Because most of the entries in the diagonal matrices F_q are “naturally” hierarchical (for UV-localized fermions), the physical fermion mass matrices m_u and m_d will inherit their hierarchical structure independently of the nature of the true 5D Yukawa couplings Y_u and Y_d , which can therefore contain all of its entries with similar size (of order 1) and have no definite flavor structure. This is the main idea behind scenarios of so-called “flavor anarchy”, which we will consider also here, but applied to a four-family scenario.

To diagonalize the mass matrices we use

$$U_{Q_u} \mathbf{m}_u W_u^\dagger = \mathbf{m}_u^{\text{diag}}, \quad (15)$$

$$U_{Q_d} \mathbf{m}_d W_d^\dagger = \mathbf{m}_d^{\text{diag}}. \quad (16)$$

One can in fact obtain a relatively simple formulation of the rotation matrices U_{Q_u} , U_{Q_d} , W_u and W_d by expanding their entries in powers of ratios f_i/f_j , where $i < j$ and with $i = 1, 2$ and $j = 1, 2, 3, 4$. Keeping only the leading terms, we obtain for U_{Q_u} , U_{Q_d} (see [22] for the three family case):

$$U_{Q_u} = \begin{pmatrix} 1 & \frac{[Y_u]_{21}}{[Y_u]_{11}} \frac{f_{Q_1}}{f_{Q_2}} & \mathcal{U}_{13}^{Q_u} & \mathcal{U}_{14}^{Q_u} \\ -\frac{[Y_u]_{21}^*}{[Y_u]_{11}^*} \frac{f_{Q_1}}{f_{Q_2}} & 1 & \mathcal{U}_{23}^{Q_u} & \mathcal{U}_{24}^{Q_u} \\ \frac{[Y_u]_{31}^*}{[Y_u]_{11}^*} \frac{f_{Q_1}}{f_{Q_3}} & -\frac{[Y_u]_{11,32}^*}{[Y_u]_{11,22}^*} \frac{f_{Q_2}}{f_{Q_3}} & \cos \theta_{Q_u} & \sin \theta_{Q_u} \\ -\frac{[Y_u]_{41}^*}{[Y_u]_{11}^*} \frac{f_{Q_1}}{f_{Q_4}} & \frac{[Y_u]_{11,42}^*}{[Y_u]_{11,22}^*} \frac{f_{Q_2}}{f_{Q_4}} & -\sin^* \theta_{Q_u} & \cos^* \theta_{Q_u} \end{pmatrix}, \quad (17)$$

and similarly for $Q_u \rightarrow Q_d$; and for the right-handed quark mixing matrix W_u :

$$W_u = \begin{pmatrix} 1 & \frac{[Y_u]_{12}^*}{[Y_u]_{11}^*} \frac{f_{u1}}{f_{u2}} & \mathcal{W}_{13}^u & \mathcal{W}_{14}^u \\ -\frac{[Y_u]_{12}}{[Y_u]_{11}} \frac{f_{u1}}{f_{u2}} & 1 & \mathcal{W}_{23}^u & \mathcal{W}_{24}^u \\ \frac{[Y_u]_{13}}{[Y_u]_{11}} \frac{f_{u1}}{f_{u3}} & -\frac{[Y_u]_{11,23}}{[Y_u]_{11,22}} \frac{f_{u2}}{f_{u3}} & \cos^* \theta_u & \sin^* \theta_u \\ -\frac{[Y_u]_{14}}{[Y_u]_{11}} \frac{f_{u1}}{f_{u4}} & \frac{[Y_u]_{11,24}}{[Y_u]_{11,22}} \frac{f_{u2}}{f_{u4}} & -\sin \theta_u & \cos \theta_u \end{pmatrix}, \quad (18)$$

with similar expression for $u \rightarrow d$.

Using the definition of the fermion mixing matrix V_{CKM}

$$V_{CKM} = U_{Q_u}^\dagger U_{Q_d}, \quad (19)$$

we can obtain obtain for example a simple expression for V_{us} as

$$V_{us} = \frac{f_{Q_1}}{f_{Q_2}} \left(\frac{[Y_d]_{21}}{[Y_d]_{11}} - \frac{[Y_u]_{21}}{[Y_u]_{11}} \right). \quad (20)$$

Similar expression can be obtained for other CKM mixing angles, as shown in [17]. Since the 5D Yukawa matrix elements are expected to be all of order 1, the observed hierarchies among the CKM elements can be explained by hierarchies among the f_i parameters.

IV. FLAVOR-CHANGING NEUTRAL COUPLINGS OF THE RADION

The couplings between bulk SM fermions and the radion were calculated in [10] for the case of one generation. Including the flavor structure and the possibility of a bulk Higgs, these couplings are the same for four generations as in the three-generation case, presented in [11] and take the form of Eq. (9). After diagonalization of the fermion mass matrix, flavor violating couplings will be generated. One can see this explicitly by performing the bi-unitary rotation leading to the fermion mass basis, and writing the radion couplings to fermions in that basis (in matrix form):

$$-\frac{\phi(x)}{\Lambda_\phi} \bar{\mathbf{d}}_L^{phys} \left[U_{qL}^\dagger \hat{\mathcal{I}}_q U_{qL} \hat{m}_d^{diag} + \hat{m}_d^{diag} W_{dR}^\dagger \hat{\mathcal{I}}_d W_{dR} \right] \mathbf{d}_R^{phys}. \quad (21)$$

Here, \mathbf{d}^{phys} is the physical state and is now a 4-vector in flavor space, given that we have introduced an extra fourth generation. Also we have defined $\hat{\mathcal{I}}_q = \text{diag}[\mathcal{I}(c_{q_i})]$ and $\hat{\mathcal{I}}_d = \text{diag}[\mathcal{I}(c_{d_i})]$. One observes that unless the diagonal matrices $\hat{\mathcal{I}}_q$ and $\hat{\mathcal{I}}_d$ are both proportional to the unit matrix,¹ there must be some degree of flavor misalignment in the radion couplings.

¹ Note that this can easily be achieved if the bulk mass parameters, the c_i 's, are all degenerate, but then the scenario cannot be used to produce/explain fermion hierarchies.

The extension to the up quark sector and charged leptons is immediate.

A. Radion FCNC's in Flavor Anarchy–Analytical Results

We explicitly parametrize the radion couplings with fermions by showing the mass dependence as

$$\mathcal{L}_{q,FV} = -\frac{\tilde{a}_{ij}^d}{\Lambda_\phi} \sqrt{m_{d_i} m_{d_j}} \phi \bar{d}_L^i d_R^j - \frac{\tilde{a}_{ij}^u}{\Lambda_\phi} \sqrt{m_{u_i} m_{u_j}} \phi \bar{u}_L^i u_R^j + \text{h.c.}, \quad (22)$$

where d^i, u^i are the quark mass eigenstates with masses m_{d_i}, m_{u_i} . Due to the simplicity of the flavor structure in the radion couplings, it is now possible to give analytical expressions for these couplings, to leading order in ratios of f_i/f_j . The general expressions are, for $i < j$:

$$\begin{aligned} \tilde{a}_{ij}^d &= \sqrt{\frac{m_{d_j}}{m_{d_i}}} \sum_{k=1}^3 \left[(\mathcal{I}(c_{q_k}) - \mathcal{I}(c_{q_4})) U_{ki}^{Q_d^*} U_{kj}^{Q_d} \right] + \mathcal{O}\left(\frac{m_{d_i}}{m_{d_j}}\right), \\ \tilde{a}_{ij}^u &= \sqrt{\frac{m_{u_j}}{m_{u_i}}} \sum_{k=1}^3 \left[(\mathcal{I}(c_{q_k}) - \mathcal{I}(c_{q_4})) U_{ki}^{Q_u^*} U_{kj}^{Q_u} \right] + \mathcal{O}\left(\frac{m_{u_i}}{m_{u_j}}\right), \end{aligned} \quad (23)$$

and for $i > j$:

$$\begin{aligned} \tilde{a}_{ij}^d &= \sqrt{\frac{m_{d_i}}{m_{d_j}}} \sum_{k=1}^3 \left[(\mathcal{I}(c_{d_k}) - \mathcal{I}(c_{d_4})) W_{ki}^d W_{kj}^{d*} \right] + \mathcal{O}\left(\frac{m_{d_j}}{m_{d_i}}\right), \\ \tilde{a}_{ij}^u &= \sqrt{\frac{m_{u_i}}{m_{u_j}}} \sum_{k=1}^3 \left[(\mathcal{I}(c_{u_k}) - \mathcal{I}(c_{u_4})) W_{ki}^u W_{kj}^{u*} \right] + \mathcal{O}\left(\frac{m_{u_j}}{m_{u_i}}\right). \end{aligned} \quad (24)$$

Note that when $i < j$ the couplings are controlled by “left-handed” bulk masses (c_q) and mixings (U^Q), and when $i > j$, the couplings are controlled by “right-handed” bulk masses ($c_{u,d}$) and mixings ($W^{u,d}$). The resulting 3×3 substructure of these couplings, i.e. without the fourth generation, match the results presented in [11].

The expansion of the mixing angles in terms of ratios of f 's gives $U_{ij}^{Q_{(d,u)}} \sim f_{Q_i}/f_{Q_j}$, $W_{ij}^d \sim f_{d_i}/f_{d_j}$, and $W_{ij}^u \sim f_{u_i}/f_{u_j}$. With these, we can obtain the parametric dependence of the radion couplings up to corrections of order one.²

The diagonal terms are simply

$$\tilde{a}_{ii}^d \approx \mathcal{I}(c_{q_i}) + \mathcal{I}(c_{d_i}), \quad \tilde{a}_{ii}^u \approx \mathcal{I}(c_{q_i}) + \mathcal{I}(c_{u_i}). \quad (25)$$

As the function $\mathcal{I}(c)$, defined in Eq. (10), tends to c for $c > 1/2$, and approaches quickly the value $1/2$ for $c < 1/2$, the diagonal terms in the down sector can be written as

$$\tilde{a}_{11}^d \approx (c_{q_1} + c_{d_1}), \quad \tilde{a}_{22}^d \approx (c_{q_2} + c_{d_2}), \quad \tilde{a}_{33}^d \approx \left(\frac{1}{2} + c_{d_3}\right), \quad \tilde{a}_{44}^d \approx 1,$$

² See Appendix for details.

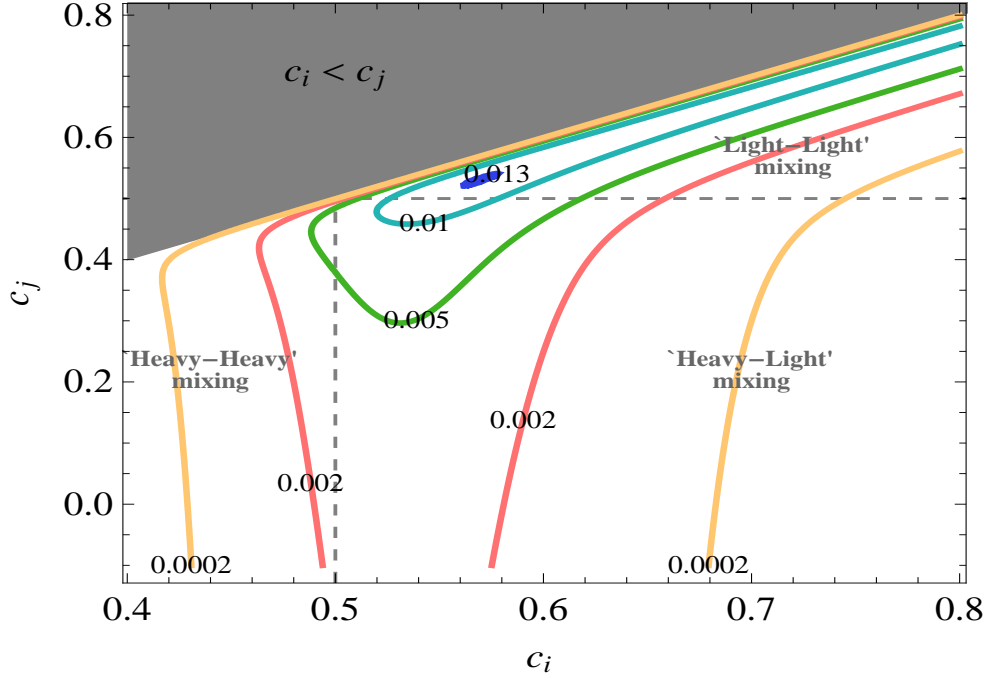


FIG. 1: Contours in the plane (c_i, c_j) of the function $\hat{a}_{ij} = [\mathcal{I}(c_i) - \mathcal{I}(c_j)] \frac{f(c_i)}{f(c_j)}$, which sets the size of radion FCNC couplings with fermions. These are estimated to be $\tilde{a}_{ij} \simeq \sqrt{\frac{m_i}{m_j}} \hat{a}_{ij}$ and so from these contours one can quickly estimate the size of these couplings by knowing the values of the bulk mass parameter c_i of each fermion.

while the off-diagonal terms also get very simple expressions

$$\begin{aligned}
\tilde{a}_{12}^d &\approx \sqrt{\frac{m_s}{m_d}} (c_{q_1} - c_{q_2}) \frac{f_{Q_1}}{f_{Q_2}}, & \tilde{a}_{21}^d &\approx \sqrt{\frac{m_s}{m_d}} (c_{d_1} - c_{d_2}) \frac{f_{d_1}}{f_{d_2}}, \\
\tilde{a}_{13}^d &\approx \sqrt{\frac{m_b}{m_d}} \left(c_{q_1} - \frac{1}{2}\right) \frac{f_{Q_1}}{f_{Q_3}}, & \tilde{a}_{31}^d &\approx \sqrt{\frac{m_b}{m_d}} (c_{d_1} - c_{d_3}) \frac{f_{d_1}}{f_{d_3}}, \\
\tilde{a}_{23}^d &\approx \sqrt{\frac{m_b}{m_s}} \left(c_{q_2} - \frac{1}{2}\right) \frac{f_{Q_2}}{f_{Q_3}}, & \tilde{a}_{32}^d &\approx \sqrt{\frac{m_b}{m_s}} (c_{d_2} - c_{d_3}) \frac{f_{d_2}}{f_{d_3}}, \\
\tilde{a}_{14}^d &\approx \sqrt{\frac{m_{b'}}{m_d}} \left(c_{q_1} - \frac{1}{2}\right) \frac{f_{Q_1}}{f_{Q_4}}, & \tilde{a}_{41}^d &\approx \sqrt{\frac{m_{b'}}{m_d}} \left(c_{d_1} - \frac{1}{2}\right) \frac{f_{d_1}}{f_{d_4}}, \\
\tilde{a}_{24}^d &\approx \sqrt{\frac{m_{b'}}{m_s}} \left(c_{q_2} - \frac{1}{2}\right) \frac{f_{Q_2}}{f_{Q_4}}, & \tilde{a}_{42}^d &\approx \sqrt{\frac{m_{b'}}{m_s}} \left(c_{d_2} - \frac{1}{2}\right) \frac{f_{d_2}}{f_{d_4}}, \\
\tilde{a}_{34}^d &\approx \sqrt{\frac{m_{b'}}{m_b}} [\mathcal{I}(c_{q_3}) - \mathcal{I}(c_{q_4})] \frac{f_{Q_3}}{f_{Q_4}}, & \tilde{a}_{43}^d &\approx \sqrt{\frac{m_{b'}}{m_s}} \left(c_{d_3} - \frac{1}{2}\right) \frac{f_{d_3}}{f_{d_4}}.
\end{aligned} \tag{26}$$

Note that in the above we took $c_{q_3} \approx c_{q_4} \approx c_{d_4} = 1/2$ except in \tilde{a}_{34}^d where the dominant term comes from the (expected small) difference between c_{q_4} and c_{q_3} .

Similarly, in the up sector, we obtain

$$\tilde{a}_{11}^u \approx (c_{q_1} + c_{u_1}), \quad \tilde{a}_{22}^u \approx (c_{q_2} + c_{u_2}), \quad \tilde{a}_{33}^u \approx 1, \quad \tilde{a}_{44}^u \approx 1,$$

and for the off-diagonal terms:

$$\begin{aligned}
\tilde{a}_{12}^u &\approx \sqrt{\frac{m_c}{m_u}} (c_{q_1} - c_{q_2}) \frac{f_{Q_1}}{f_{Q_2}}, & \tilde{a}_{21}^u &\approx \sqrt{\frac{m_c}{m_u}} (c_{u_1} - c_{u_2}) \frac{f_{u_1}}{f_{u_2}}, \\
\tilde{a}_{13}^u &\approx \sqrt{\frac{m_t}{m_u}} \left(c_{q_1} - \frac{1}{2}\right) \frac{f_{Q_1}}{f_{Q_3}}, & \tilde{a}_{31}^u &\approx \sqrt{\frac{m_t}{m_u}} \left(c_{u_1} - \frac{1}{2}\right) \frac{f_{d_1}}{f_{d_3}}, \\
\tilde{a}_{23}^u &\approx \sqrt{\frac{m_t}{m_c}} \left(c_{q_2} - \frac{1}{2}\right) \frac{f_{Q_2}}{f_{Q_3}}, & \tilde{a}_{32}^u &\approx \sqrt{\frac{m_t}{m_c}} \left(c_{u_2} - \frac{1}{2}\right) \frac{f_{u_2}}{f_{u_3}}, \\
\tilde{a}_{14}^u &\approx \sqrt{\frac{m_{t'}}{m_u}} \left(c_{q_1} - \frac{1}{2}\right) \frac{f_{Q_1}}{f_{Q_4}}, & \tilde{a}_{41}^u &\approx \sqrt{\frac{m_{t'}}{m_u}} \left(c_{u_1} - \frac{1}{2}\right) \frac{f_{u_1}}{f_{u_4}}, \\
\tilde{a}_{24}^u &\approx \sqrt{\frac{m_{t'}}{m_c}} \left(c_{q_2} - \frac{1}{2}\right) \frac{f_{Q_2}}{f_{Q_4}}, & \tilde{a}_{42}^u &\approx \sqrt{\frac{m_{t'}}{m_c}} \left(c_{u_2} - \frac{1}{2}\right) \frac{f_{u_2}}{f_{u_4}}, \\
\tilde{a}_{34}^u &\approx \sqrt{\frac{m_{t'}}{m_t}} [\mathcal{I}(c_{q_3}) - \mathcal{I}(c_{q_4})] \frac{f_{Q_3}}{f_{Q_4}}, & \tilde{a}_{43}^u &\approx \sqrt{\frac{m_{t'}}{m_t}} (\mathcal{I}(c_{u_3}) - \mathcal{I}(c_{u_4})) \frac{f_{u_3}}{f_{u_4}}.
\end{aligned} \tag{27}$$

Here we assumed $c_{q_3} \approx c_{q_4} \approx c_{u_3} \approx c_{u_4} = 1/2$ except in $\tilde{a}_{34}^u, \tilde{a}_{43}^u$, for the same reasons given for the down sector. This situation is very different from the case of FCNC couplings of the Higgs boson [17] where the couplings a_{34}, a_{43} are large due to significant misalignment in the 3-4 family. It is clear from the expressions for $\tilde{a}_{ij}^d, \tilde{a}_{ij}^u$ that the flavor changing couplings of the radion are of the simple form $\sqrt{\frac{m_j}{m_i}} [\mathcal{I}(c_i) - \mathcal{I}(c_j)] \frac{f_i}{f_j}$. We explore typical values of this function as contours in a c_i, c_j plane, and determine the localization coefficients for which this function is maximal. In Fig. 1, we show contours of the in the plane of the \tilde{a}_{ij} as a function of two bulk mass parameters, (c_i, c_j) for $c_i < c_j$. The light-light regions correspond to mixing among the first two families, and b_R . Corresponding to localization of light quarks these are maximal and the FCNC couplings of the radion \tilde{a}_{ij} can reach a maximum of 0.013. The heavy-light mixing correspond to the fourth family mixing, or third family doublet, or t_R mixing, with the light two families and b_R . These mixings can reach 0.01, although they are more likely to be in the $(0.002 - 0.005)$ region. Finally the heavy-heavy mixing (among fourth families, $(t b)_L$ and u_R) can reach 0.02 as c_{q_3}, c_{u_3} deviate from $1/2$. The results of the analytic calculations agree with our numerical scan presented in the next subsection.

B. Radion FCNC's in Flavor Anarchy–Numerical Results

We complement our analytical consideration by performing a numerical scan over the parameter space. We proceed as follows. We generate random complex entries for Y_u and Y_d , then obtain values for f_{u_i}, f_{d_i} and f_{Q_i} in the same way as for the Higgs FCNC couplings [17], in matrix form. Using $f(c)$ from Eq. (14), we solve for the coefficients c_i . We then use the expression for $\mathcal{I}(c_i)$ to calculate mass matrices $\hat{\mathbf{m}}_{\mathbf{u}}, \hat{\mathbf{m}}_{\mathbf{d}}$, then obtain the eigenvalues, and the matrices $W_{u,d}$ and $U_{Q_{u,d}}$. We then have all the ingredients to calculate the fermion-radion

couplings. From the scan in parameter space, we find the $\tilde{a}_{ij}^d, \tilde{a}_{ij}^u$ as follows

$$\tilde{a}_{ij}^d \sim \begin{pmatrix} 1.295 - 1.315 & 0.017 - 0.039 & 0.010 - 0.025 & 0.089 - 0.290 \\ 0.013 - 0.034 & 1.215 - 1.231 & 0.006 - 0.016 & 0.065 - 0.179 \\ 0.080 - 0.201 & 0.016 - 0.050 & 1.129 - 1.151 & 0.0002 - 0.001 \\ 0.024 - 0.076 & 0.018 - 0.049 & 0.004 - 0.012 & 1.000 - 1.001 \end{pmatrix}, \quad (28)$$

$$\tilde{a}_{ij}^u \sim \begin{pmatrix} 1.294 - 1.320 & 0.065 - 0.164 & 0.081 - 0.212 & 0.094 - 0.268 \\ 0.022 - 0.055 & 1.135 - 1.158 & 0.019 - 0.047 & 0.019 - 0.053 \\ 0.030 - 0.098 & 0.042 - 0.103 & 1.002 - 1.016 & 0.0003 - 0.002 \\ 0.023 - 0.078 & 0.030 - 0.075 & 0.001 - 0.005 & 1.000 - 1.002 \end{pmatrix}. \quad (29)$$

The above ranges show the 50% quantile of acceptable points, which means that 25% of points found predict lower $\tilde{a}_{ij}^d, \tilde{a}_{ij}^u$ values and 25% of points predict higher values than those shown in the matrices. The results of the scan are consistent with the values obtained through analytical considerations and from the values estimated using Fig. 1, once typical sizes of the bulk masses are associated to the appropriate fermions.

C. Radion FCNC's in Flavor Anarchy-Leptons

We proceed in a similar fashion to calculate the FCNC couplings of the radion with the leptons. Assuming the neutrinos to be Dirac-type, we parametrize the couplings as

$$\mathcal{L}_{l,FV} = -\frac{\tilde{a}_{ij}^l}{\Lambda_\phi} \sqrt{m_{l_i} m_{l_j}} \phi \bar{l}_L^i l_R^j - \frac{\tilde{a}_{ij}^\nu}{\Lambda_\phi} \sqrt{m_{\nu_i} m_{\nu_j}} \phi \bar{\nu}_L^i \nu_R^j + \text{h.c.} \quad (30)$$

The couplings of the charged leptons will resemble those of the down-type quarks, the only difference being that $c_{L_3} \neq \frac{1}{2}$. The coefficients c_{L_i} , $i = 1, 2, 3$ are very close and can be large, while $c_{L_4} = \frac{1}{2}$. The matrix $\hat{\mathcal{I}}_L = \text{diag}[\mathcal{I}(c_{L_j})]$, $j = 1, 2, 3, 4$ in Eq. 9 can be written as a diagonal matrix plus a non-diagonal one, with entries $\text{diag}(0, 0, 0, \Delta c)$, where $\Delta c = c_{L_4} - c_{L_i}$ can be large.

As the neutrinos are massless, the only FCNC non-zero couplings involve the fourth family, that is $\tilde{a}_{ij}^\nu \neq 0$ only if either $i = 4$ and/or $j = 4$. While couplings with quark are restricted by the CKM matrix (its 3×3 substructure), the lepton mixing matrix U^{PMNS} is not as well known, and thus restrictions on the U_{i4}^{PMNS} , U_{4j}^{PMNS} are even less established. We assume that the left-handed matrix U^L is hierarchical, thus almost diagonal and U^ν nonhierarchical, and almost the same as U^{PMNS} .

This would imply the same type of parametric dependence as in the quark sector:

$$\tilde{a}_{14}^\nu = \sqrt{\frac{m_{\nu_4}}{m_{\nu_1}}} [c_{L_1} - \mathcal{I}(c_{L_4})] \frac{f_{L_1}}{f_{L_4}} \mathcal{O}(1),$$

$$\begin{aligned}\tilde{a}_{24}^\nu &= \sqrt{\frac{m_{\nu_4}}{m_{\nu_2}}} [c_{L_2} - \mathcal{I}(c_{L_4})] \frac{f_{L_2}}{f_{L_4}} \mathcal{O}(1), \\ \tilde{a}_{34}^\nu &= \sqrt{\frac{m_{\nu_4}}{m_{\nu_3}}} [c_{L_3} - \mathcal{I}(c_{L_4})] \frac{f_{L_3}}{f_{L_4}} \mathcal{O}(1),\end{aligned}\tag{31}$$

where the coefficients c_{L_i} describe the localization of the lepton doublets and can be large, and f_{L_i} are the values of the zero-mode wavefunctions for the doublet lepton i at the IR brane. For the right-handed neutrinos, W^ν is almost diagonal to insure small neutrino masses. Thus \tilde{a}_{4j} , $j \neq 4$ are small and can be neglected. Here the dominant term could be \tilde{a}_{34}^ν . For $c_{L_i}, c_{\nu_i} > 1/2$, the zero modes wavefunctions are localized towards the UV brane; if $c_{L_i}, c_{\nu_i} < 1/2$, they are localized towards the IR brane. However the size of \tilde{a}_{34}^ν is also determined by the mixing terms $U_{33}^L U_{34}^{L*}$, as given in Eq. (39). Thus the mixing will be proportional to $f(c) \equiv \sqrt{\frac{1-2c}{1-\epsilon^{1-2c}}}$ where the hierarchically small parameter $\epsilon = R/R' \approx 10^{-15}$ is generally referred to as the warp factor. Thus, we must choose a value for c_{L_3} which maximizes the expression $\tilde{a}_{34}^\nu \approx [\mathcal{I}(c_{L_3} - \mathcal{I}(c_{L_4}))] f(c_{L_3})$. These values correspond to the region of Fig. 1 for the light-heavy region.

V. PHENOMENOLOGY

A. Bounds on Radion-mediated FCNC couplings

The off-diagonal Yukawa couplings induce FCNC in both quark and lepton interactions, which affect low energy observables and also give possible signatures at colliders. In this section, we discuss restrictions on radion flavor violation coming from tree-level processes $\Delta F = 2$, such as $K - \bar{K}$, $B - \bar{B}$, $D - \bar{D}$ mixing. We use an effective Lagrangian approach [24, 25] to isolate the contributions. The $\Delta F = 2$ process are described by the Hamiltonian [26, 27]

$$\mathcal{H}_{eff}^{\Delta F=2} = \sum_{a=1}^5 C_a Q_a^{q_i q_j} + \sum_{a=1}^3 \tilde{C}_a \tilde{Q}_a^{q_i q_j},\tag{32}$$

with

$$\begin{aligned}Q_1^{q_i q_j} &= \bar{q}_{jL}^\alpha \gamma_\mu q_{iL}^\alpha \bar{q}_{jL}^\beta \gamma^\mu q_{iL}^\beta, & Q_2^{q_i q_j} &= \bar{q}_{jR}^\alpha q_{iL}^\alpha \bar{q}_{jR}^\beta q_{iL}^\beta, & Q_3^{q_i q_j} &= \bar{q}_{jR}^\alpha q_{iL}^\beta \bar{q}_{jR}^\beta q_{iL}^\alpha, \\ Q_4^{q_i q_j} &= \bar{q}_{jR}^\alpha q_{iL}^\alpha \bar{q}_{jL}^\beta q_{iR}^\beta, & Q_5^{q_i q_j} &= \bar{q}_{jR}^\alpha q_{iL}^\beta \bar{q}_{jL}^\beta q_{iR}^\alpha,\end{aligned}\tag{33}$$

where α, β are color indices. The operators \tilde{Q}_a are obtained from Q_a by exchange $L \leftrightarrow R$. For $K - \bar{K}$, $B_d - \bar{B}_d$, $B_s - \bar{B}_s$, $D - \bar{D}$ mixing, $q_i q_j = sd, bd, bs$ and uc respectively.

Exchange of the flavor-violating radions gives rise to additional contributions to C_2 , \tilde{C}_2 and C_4 operators. These are given below, using the model-independent bounds on BSM

contributions as in [27] to present coupled constraints on \tilde{a}_{ij} couplings and the radion mass m_ϕ .

At the scale $m_\phi = 60$ GeV, the limits on the C_2 , \tilde{C}_2 and C_4 operators are:

$$\begin{aligned}
\text{Re}C_K^2 &\leq \left(\frac{1}{5.3 \times 10^6 \text{ GeV}}\right)^2, & \text{Re}C_K^4 &\leq \left(\frac{1}{9.1 \times 10^6 \text{ GeV}}\right)^2, \\
\text{Im}C_K^2 &\leq \left(\frac{1}{9.5 \times 10^7 \text{ GeV}}\right)^2, & \text{Im}C_K^4 &\leq \left(\frac{1}{1.2 \times 10^8 \text{ GeV}}\right)^2, \\
|C_D^2| &\leq \left(\frac{1}{1.8 \times 10^6 \text{ GeV}}\right)^2, & |C_D^4| &\leq \left(\frac{1}{2.6 \times 10^6 \text{ GeV}}\right)^2, \\
|C_{B_d}^2| &\leq \left(\frac{1}{8.7 \times 10^5 \text{ GeV}}\right)^2, & |C_{B_d}^4| &\leq \left(\frac{1}{1.3 \times 10^6 \text{ GeV}}\right)^2, \\
|C_{B_s}^2| &\leq \left(\frac{1}{1.0 \times 10^5 \text{ GeV}}\right)^2, & |C_{B_s}^4| &\leq \left(\frac{1}{1.6 \times 10^5 \text{ GeV}}\right)^2.
\end{aligned} \tag{34}$$

Using these bounds we obtain the constraints on radion flavor violating Yukawa couplings (as compared to the \tilde{a}_{ij} in the scan)

$$\begin{aligned}
\Omega^2 \text{Re}(\tilde{a}_{12}^{d*})^2 &\leq 2.6, & \Omega^2 \text{Re}(\tilde{a}_{21}^d)^2 &\leq 2.6, & \Omega^2 \text{Re}(\tilde{a}_{12}^{d*} \tilde{a}_{21}^d) &\leq 0.90, \\
\Omega^2 \text{Im}(\tilde{a}_{12}^{d*})^2 &\leq 0.0082, & \Omega^2 \text{Im}(\tilde{a}_{21}^d)^2 &\leq 0.0082, & \Omega^2 \text{Im}(\tilde{a}_{12}^{d*} \tilde{a}_{21}^d) &\leq 0.0050, \\
\Omega^2 |\tilde{a}_{13}^{u*}|^2 &\leq 3.2, & \Omega^2 |\tilde{a}_{31}^u|^2 &\leq 3.2, & \Omega^2 |\tilde{a}_{31}^{u*} \tilde{a}_{13}^u| &\leq 1.4, \\
\Omega^2 |\tilde{a}_{13}^{d*}|^2 &\leq 1.9, & \Omega^2 |\tilde{a}_{31}^d|^2 &\leq 1.9, & \Omega^2 |\tilde{a}_{13}^{d*} \tilde{a}_{31}^d| &\leq 0.87, \\
\Omega^2 |\tilde{a}_{32}^{d*}|^2 &\leq 6.5, & \Omega^2 |\tilde{a}_{23}^d|^2 &\leq 6.5, & \Omega^2 |\tilde{a}_{32}^{d*} \tilde{a}_{23}^d| &\leq 2.8,
\end{aligned} \tag{35}$$

where $\Omega = \left(\frac{60 \text{ GeV}}{m_\phi}\right) \left(\frac{2 \text{ TeV}}{\Lambda_\phi}\right)$. Using our analytic results, the bounds translate parametrically on restrictions on the bulk mass parameters of the appropriate fermions. From the ϵ_K bounds

$$\begin{aligned}
\text{Im}(\tilde{a}_{12}^{d*} \tilde{a}_{21}^d) &= -\frac{m_s}{m_d} (c_{q_1} - c_{q_2})(c_{d_1} - c_{d_2}) \frac{f_{Q_1} f_{d_1}}{f_{Q_2} f_{d_2}} \text{Im} \left(\frac{[Y_d]_{21}^* [Y_d]_{12}^*}{([Y_d]_{11}^*)^2} \right) \\
&= \mathcal{O}(1)(c_{q_1} - c_{q_2})(c_{d_1} - c_{d_2}),
\end{aligned} \tag{36}$$

where in the last expression we used the hierarchic nature of the Yukawa couplings.³ This is a remarkable result, as it relates the magnitude of ϵ_K directly to the bulk mass parameters (or the localization coefficients) of the d , s quarks in the $U(1)_R$ singlet and $SU(2)_L$ doublet representations. Similarly we can obtain appropriate expressions to obtain parametric restrictions on the bulk mass parameters coming from $B^0 - \bar{B}^0$ and $D^0 - \bar{D}^0$ mixing:

$$\begin{aligned}
|\tilde{a}_{13}^{d*} \tilde{a}_{31}^d| &= \mathcal{O}(1)(c_{q_1} - \frac{1}{2})(c_{d_1} - c_{d_3}), \\
|\tilde{a}_{32}^{d*} \tilde{a}_{23}^d| &= \mathcal{O}(1)(c_{q_2} - \frac{1}{2})(c_{d_2} - c_{d_3}), \\
|\tilde{a}_{13}^{u*} \tilde{a}_{31}^u| &= \mathcal{O}(1)(c_{q_1} - \frac{1}{2})(c_{d_1} - \frac{1}{2}).
\end{aligned} \tag{37}$$

³ See Appendix for details.

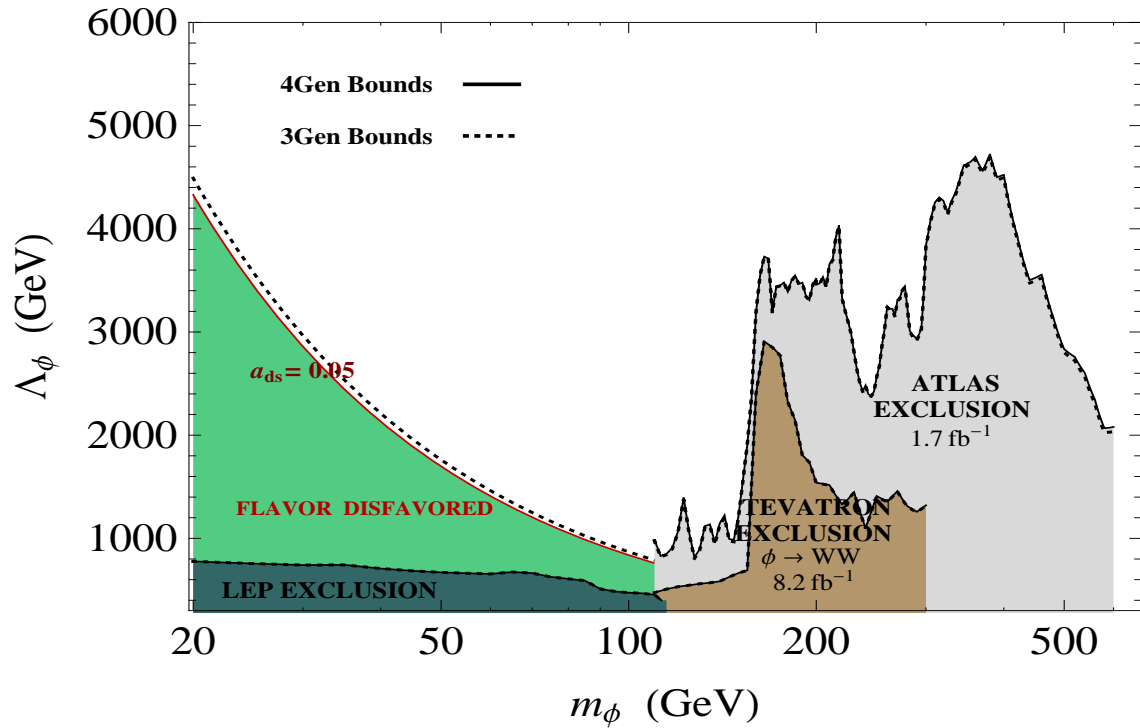


FIG. 2: Restrictions in the $m_\phi - \Lambda_\phi$ plane from collider exclusion limits and flavor constraints for ϵ_K (we have defined $a_{ds} = \sqrt{\text{Im}(\tilde{a}_{12}^{d*}\tilde{a}_{21}^d)}$). One sees that for lighter radion ($m_\phi < 160$ GeV) direct bounds are quite weak and flavor physics provide stronger constraints (although less robust). Heavier radions are mostly constrained by the “golden mode” $pp \rightarrow \phi \rightarrow ZZ$ and also $pp \rightarrow \phi \rightarrow WW$ at the LHC, while $p\bar{p} \rightarrow \phi \rightarrow WW$ is used at Tevatron.

One can see from the bounds, that unless the radion is very light ($m_\phi \sim 10$ GeV), the most significant constraints come from the ϵ_K bounds, especially those on the coefficient C_4 . We thus use these bounds as the main flavor constraints on our model, and present the restrictions in Fig. 2 in the $m_\phi - \Lambda_\phi$ plane (for the typical value of $\tilde{a}_{12}^d \sim \tilde{a}_{21}^d \sim 0.05$). The region below the $a_{ds} = 0.05$ curve is thus named “flavor disfavored”, since typical flavor anarchy parameter points would produce too large contributions to ϵ_K in that region. Note that we considered the scenarios with both 3 and 4 generations of fermions, and the bounds are basically the same. The small difference is due to the renormalization group running of operators, which is slightly altered by the presence of extra fermion families.

In the same figure we present the most recent direct bounds on radion phenomenology coming from collider data. Indeed one can easily use the existing Higgs bounds to restrict regions in the $m_\phi - \Lambda_\phi$ plane, since the search strategy for both the Higgs and the radion are identical. This is due to the fact that the couplings of the radion with matter particles are proportional to the mass of the particles (just like the couplings of the Higgs). The main difference is that the Higgs couplings are controlled by the electroweak scale v , whereas the radion couplings are controlled (suppressed) by the much heavier scale Λ_ϕ .

LEP bounds [28] do apply for very light radion, although the restrictions on Λ_ϕ are not too strong, and one sees that in that region the generic flavor bounds are much stronger (although less robust).

For heavier radion, the Tevatron and very recently the LHC do put strong bounds in the allowed parameter region of our scenario. In both experiments, the main production mechanism for the radion is via gluon fusion but, unlike the Higgs, the other possible production mechanisms such as vector boson fusion or associated W and Z production are extremely suppressed. This is due to the special enhancement of the coupling of radion to gluons through the trace anomaly. The consequence of this fact is that Higgs searches must be appropriately translated into radion bounds by subtracting events coming from scalars produced via vector boson fusion. One can do this roughly by adjusting the production cross section of the Higgs in order to only obtain the gluon fusion cross section. A better way of translating Higgs searches into radion is to use fourth generation Higgs searches. This is because a Higgs with 4 generations will mainly be produced in gluon fusion (with almost no other production channel) and so there will be no need of subtracting events coming from other production mechanisms.

Another important issue when translating Higgs bounds is that the width of a heavier Higgs ($m_h > 200\text{GeV}$) starts to be relevant (i.e. becomes larger than the experimental resolution). This means that more background events must be integrated in order to optimize signal events. But the radion width is always going to remain much smaller than experimental resolution due to its couplings being suppressed by Λ_ϕ (and not v as in the Higgs case). We must therefore adjust again the Higgs limits in order to take this fact into account, since much less background events should be kept in a pure radion search [8].

With all this in mind, we translate Tevatron and LHC bounds from Higgs searches and show the excluded regions in Figure 2. From the Tevatron collider, we use the CDF and D0 combined search for a fourth generation Higgs, which allows interesting bounds up to masses of $m_\phi = 300\text{ GeV}$ [29]. This search focuses on the Higgs decay into pairs of W bosons and makes use of an integrated luminosity of 8.2 fb^{-1} . As for the LHC, we use the recent results from the ATLAS experiment [30], in which they perform a combination of different channels, with integrated luminosities up to 1.7 fb^{-1} . As one can see, LHC data from a single experiment outperforms the Tevatron and quite interesting bounds can be set up to a mass of $m_\phi = 600\text{ GeV}$. We note that because the relative importance of different channels is not exactly the same for Higgs and radion (specially the branching of the $\phi \rightarrow \gamma\gamma$ channel differs from $h \rightarrow \gamma\gamma$), in the lower mass region $m_h < 160\text{ GeV}$ we avoid the combination and use exclusively the ATLAS limits from $h \rightarrow \gamma\gamma$ search. Above that point the branchings of Higgs and radion into heavy vector bosons are essentially the same, specially if we assume for the plot that the fourth generation of fermions (if it exists) is heavy enough, with masses

greater than 300 GeV.

Finally we note from this figure that radion phenomenology does not really change due to the addition of a fourth family⁴. This might seem surprising because the Higgs phenomenology is greatly affected by the presence of a fourth family of fermions (specially fourth family quarks) due to an important enhancement in the Higgs production cross section. This does not happen in the case of the radion, because its couplings with massless gauge bosons are quite indifferent to the addition of new heavy degrees of freedom. Even though the new added fields will produce new loop contributions to $\phi \rightarrow gg$ or to $h \rightarrow \gamma\gamma$, their presence will also alter the β functions of the appropriate gauge groups, which will affect the couplings of the radion to massless bosons through the trace anomaly. The new trace anomaly effects coming from a fourth family will in fact cancel the previous loop contributions in the limit of very heavy new states [10], and so basically the radion couplings to photons and gluons remains the same, controlled only by the light degrees of freedom of the theory [31].

VI. FLAVOR CHANGING RADION DECAYS IN THE 4 GENERATION MODEL

Radion couplings to fermions, massive and massless gauge bosons have all been investigated before [10, 11]. Here we investigate the changes in branching ratios due to the effect of a fourth generation, and of flavor-changing interactions. We assume no Higgs-radion mixing. We present our results in Fig. 3. Note that we keep the radion mass to be above $\sim 5 - 10$ GeV to avoid constraints from B-meson decays and astrophysical data [32].

Depending on the masses of the fourth generation leptons and neutrinos, FCNC decay channels ($\phi \rightarrow \tau\tau'$, $\nu_\tau\nu_4$) could open for $m_\phi \geq 100\text{GeV}$. At higher radion masses, the WW, ZZ and $t\bar{t}$ dominate. In this region, the radion could be observed through the semi-leptonic channel $\phi \rightarrow W_{lep}W_{had}$, and similarly $\phi \rightarrow t\bar{t} \rightarrow b\bar{b}W_{had}W_{lep}$ (avoiding the fully hadronic channel which suffers from large QCD dijet background), but the decays rate would be comparable to that of a direct Higgs boson production.

Finally, for light (Dirac) fourth-generation neutrinos or leptons, near the present bounds, radion branching ratios to $\nu_4\nu_4$ and $\tau'\tau'$ can be significant and compete with ZZ and WW decays, and thus significantly alter radion decay patterns for $m_\phi > 200$ GeV.

⁴ We assume here that the radion decays to fourth generation fermions (especially leptons and neutrinos) is negligible. For an alternative scenario, see next section.

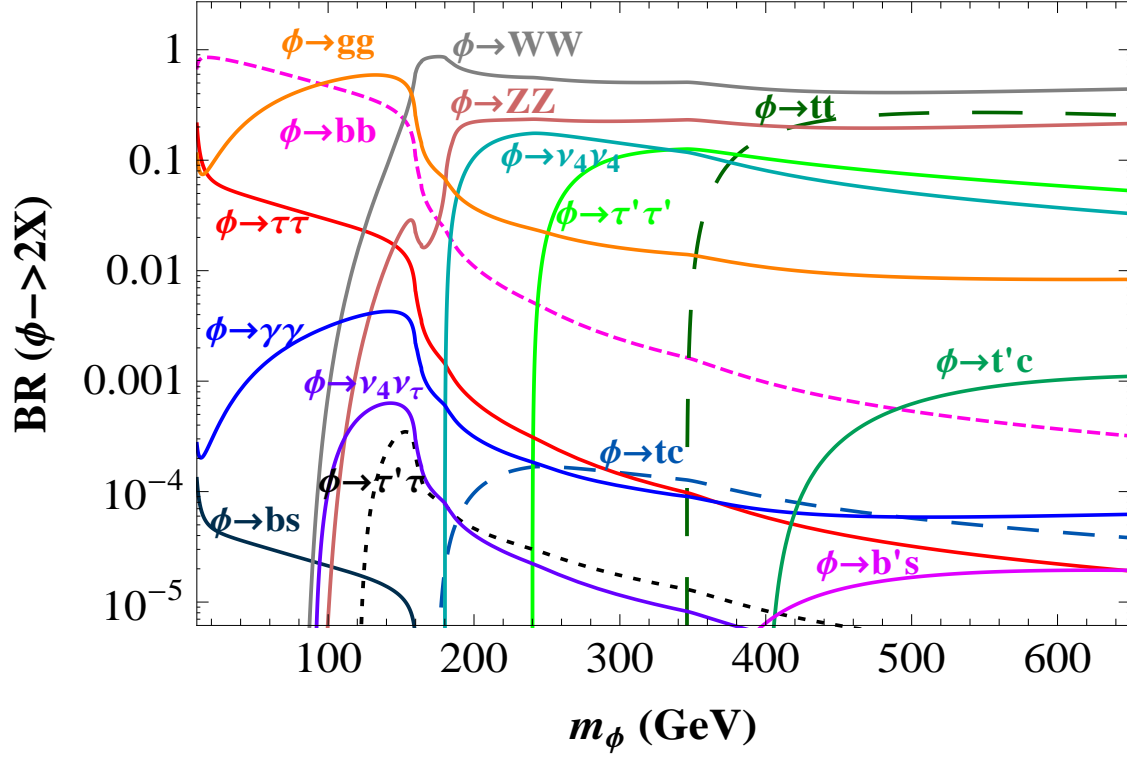


FIG. 3: Decay branching fractions of the radion in a warped scenario with four generations of fermions. The flavor anarchy setup (masses and mixings explained through fermion localization, with random 5D Yukawa couplings) predicts generic FV couplings of the radion, leading to a few new interesting decay channels such as $\phi \rightarrow bb'$ and $\phi \rightarrow \tau\tau'$. The masses chosen for this plot are $m_{b'} = 350$ GeV, $m_{t'} = 400$ GeV, $m_{\tau'} = 120$ GeV and $m_{\nu_4} = 90$ GeV, and the KK scale is $(R')^{-1} = (\sqrt{6})1500$ GeV (~ 3675 GeV).

VII. CONCLUSIONS AND OUTLOOK

In this work, we have investigated the phenomenology of the couplings, especially the flavor-violating ones, of the radion to fermions in a warped model with three and four generations where the fermions are allowed to propagate in the bulk. We have shown how to obtain these couplings analytically, and presented leading order expressions for them in a compact form. Although the radion FCNC couplings have been analyzed before, some of the analytic expressions presented here are new. We also explored the regions in which the couplings lie, and maximal values for these, as contour plots in a plane defined by coefficients describing quark localization with respect to the TeV brane. We are able to predict typical (and maximal) values for the radion coupling to heavy-heavy, light-light, and heavy-light quarks, and these results are confirmed by an extensive numerical scan.

Applying these to phenomenology of the radion, we calculated the tree-level FCNC contributions to $K^0 - \bar{K}^0$, ϵ_K , $D^0 - \bar{D}^0$ and $B^0 - \bar{B}^0$ mixing, and the restrictions imposed on the couplings. We obtain simple expressions relating quark localization to these experimental

values. The most stringent constraints are from ϵ_K , yielding a region of space in $m_\phi - \Lambda_\phi$ parameter space disfavored by flavor violation consideration. We add to these the most recent constraints on Higgs masses, from ATLAS and CMS, translating them into combined radion mass-scale limits. Our figure shows that a large range around a light radion mass-low scale ($\Lambda_\phi \sim 2$ TeV, $m_\phi \sim 60$ GeV) survives. Our analysis also shows that, unlike the case of the Higgs boson, there are minute differences between radion mass-scale limits in 3 and 4 generations, and thus these limits are quite independent of the number of generations. This conclusion stands in the case where the radion decays are not significantly influenced by decays into fourth generation fermions (in particular to fourth generation neutrinos or leptons, which have the lowest mass bounds). In a complete decay plot, we include all branching ratios of the radion. Expected to be light, the radion decays primarily to gg and $b\bar{b}$ at low masses ($m_\phi \leq 100$ GeV), while for heavier radions ($m_\phi \approx 100$ GeV), FCNC decay channel such as $\nu_4\nu_\tau$ (assuming Dirac neutrinos) and $\tau'\tau$ open, with branching ratios of 10^{-3} . These are the most promising FCNC decays of the radion, barring the unlikely appearance of $\phi \rightarrow t'c$ at the high $m_{t'} = 400$ GeV threshold. However, flavor-conserving radion decays into fourth generation leptons and neutrinos can be large (for $m_{\nu_4}, m_{\tau'} \simeq 100$ GeV) and alter the dominant decay modes for a heavier radion $r \rightarrow ZZ, WW$. These are typical decay for a radion in a model with four generations and would provide a distinguishing signal for the model. If a heavy Higgs-like state is discovered at the LHC with the usual “golden mode”, $pp \rightarrow h \rightarrow ZZ$, a width measurement could rule out a conventional Higgs boson. A careful study for different and/or exotic decay channels of that resonance might be the key to discover both a fourth generation of fermions and a warped extra dimension.

VIII. ACKNOWLEDGMENTS

M.T. would like to thank Nobuchika Okada for earlier collaboration and discussions on translating Higgs and other experimental bounds into radion bounds. M.T. would also like to thank Alex Azatov and Lijun Zhu for discussions. We acknowledge NSERC of Canada for partial financial support under grant number SAP105354.

IX. APPENDIX

In the mass basis, the radion couplings with fermions are

$$\mathcal{L}_{q,FV} = -\frac{\tilde{a}_{ij}^d}{\Lambda_\phi} \sqrt{m_{d_i} m_{d_j}} \phi \bar{d}_L^i d_R^j - \frac{\tilde{a}_{ij}^u}{\Lambda_\phi} \sqrt{m_{u_i} m_{u_j}} \phi \bar{u}_L^i u_R^j + \text{h.c.} \quad (38)$$

where d^i, u^i are the quark mass eigenstates with masses m_{d_i}, m_{u_i} . Due to the simplicity of the flavor structure in the radion couplings, it is now possible to give analytical expressions for these couplings, to leading order in ratios of f_i/f_j . In the down sector, the general expressions are, for $i < j$:

$$\tilde{a}_{ij}^d = \sqrt{\frac{m_{d_j}}{m_{d_i}}} \sum_{k=1}^3 \left[(\mathcal{I}(c_{q_k}) - \mathcal{I}(c_{q_4})) U_{ki}^{Q_d*} U_{kj}^{Q_d} \right] + \mathcal{O}\left(\frac{m_{d_i}}{m_{d_j}}\right), \quad (39)$$

and for $i > j$:

$$\tilde{a}_{ij}^d = \sqrt{\frac{m_{d_i}}{m_{d_j}}} \sum_{k=1}^3 \left[(\mathcal{I}(c_{d_k}) - \mathcal{I}(c_{d_4})) W_{ki}^d W_{kj}^{d*} \right] + \mathcal{O}\left(\frac{m_{d_j}}{m_{d_i}}\right). \quad (40)$$

where the function $\mathcal{I}(c)$ is defined by

$$\mathcal{I}(c) = \left[\frac{(\frac{1}{2} - c)}{1 - (R/R')^{1-2c}} + c \right] \approx \begin{cases} c & (c > 1/2) \\ \frac{1}{2} & (c < 1/2) \end{cases}. \quad (41)$$

Note that when $i < j$ the couplings are controlled by “left-handed” bulk masses (c_q) and mixings (U^Q), and when $i > j$, the couplings are controlled by “right-handed” bulk masses ($c_{u,d}$) and mixings ($W^{u,d}$).

We can use the previous analytical expressions for these couplings to obtain surprisingly simple parametric dependences in terms of the 5D mass parameters, up to leading order in ratios of the fermion masses m_i/m_j and of wave function profiles f_i/f_j . The final results were presented in the main text. Here we show how to extract these dependences carefully for a few terms.

We focus first on the couplings between the radion, the *down* quark and the *bottom* quark. The couplings involved are \tilde{a}_{13}^d and \tilde{a}_{31}^d . From Eq. (39) we can write explicitly

$$\begin{aligned} \tilde{a}_{13}^d = & \sqrt{\frac{m_b}{m_d}} \left[(c_{q_1} - \mathcal{I}(c_{q_4})) U_{11}^{Q_d*} U_{13}^{Q_d} + (c_{q_2} - \mathcal{I}(c_{q_4})) U_{21}^{Q_d*} U_{23}^{Q_d} \right. \\ & \left. + (\mathcal{I}(c_{q_3}) - \mathcal{I}(c_{q_4})) U_{31}^{Q_d*} U_{33}^{Q_d} \right] + \mathcal{O}\left(\frac{m_d}{m_b}\right). \end{aligned} \quad (42)$$

We have assumed explicitly that $\mathcal{I}(c_{q_1}) = c_{q_1}$ and $\mathcal{I}(c_{q_2}) = c_{q_2}$ given that the left handed down and strange quark are supposed to be UV localized. On the other hand the left handed bottom quark and the left handed b' quark are TeV brane localized, and so their bulk mass parameters c_{q_3} and c_{q_4} must be greater than 1/2, and thus we have $\mathcal{I}(c_{q_3}) \simeq \mathcal{I}(c_{q_4}) \simeq \frac{1}{2}$. We thus obtain the simpler expression (since $\mathcal{I}(c_{q_3}) - \mathcal{I}(c_{q_4}) \simeq 0$)

$$\tilde{a}_{13}^d \simeq \sqrt{\frac{m_b}{m_d}} \left[\left(c_{q_1} - \frac{1}{2}\right) U_{11}^{Q_d*} U_{13}^{Q_d} + \left(c_{q_2} - \frac{1}{2}\right) U_{21}^{Q_d*} U_{23}^{Q_d} \right]. \quad (43)$$

Finally from the dependence of mixing angles with fermion profiles, i.e $U_{ij}^{Q(d,u)} \sim f_{Q_i}/f_{Q_j}$, it is clear that the two remaining terms are of the same order $\sim f_{Q_1}/f_{Q_3}$. Since c_{q_1} is greater than c_{q_2} , we derive the parametric result presented in the main text

$$\tilde{a}_{13}^d = \sqrt{\frac{m_b}{m_d}} \left(c_{q_1} - \frac{1}{2} \right) \frac{f_{Q_1}}{f_{Q_3}} \mathcal{O}(1). \quad (44)$$

A slightly different example is the calculation for \tilde{a}_{31}^d , which we write first as

$$\begin{aligned} \tilde{a}_{31}^d = \sqrt{\frac{m_b}{m_d}} & \left[(c_{d_1} - c_{d_3}) W_{11}^d W_{13}^{d*} + (c_{d_2} - c_{d_3}) W_{21}^d W_{23}^{d*} \right. \\ & \left. + (\mathcal{I}(c_{d_4}) - c_{d_3}) W_{41}^d W_{43}^{d*} \right] + \mathcal{O}\left(\frac{m_d}{m_b}\right). \end{aligned} \quad (45)$$

One difference now is that the right handed bottom quark is UV localized and so we have $\mathcal{I}(c_{d_3}) = c_{d_3} \neq \frac{1}{2}$. Also, now $W_{41}^d W_{43}^{d*} \sim \frac{f_{d_1} f_{d_3}}{f_{d_4}^2} \ll \frac{f_{d_1}}{f_{d_3}} \sim W_{11}^d W_{13}^{d*} \sim W_{21}^d W_{23}^{d*}$ and so the expression becomes

$$\begin{aligned} \tilde{a}_{31}^d & \simeq \sqrt{\frac{m_b}{m_d}} \left[(c_{d_1} - c_{d_3}) W_{11}^d W_{13}^{d*} + (c_{d_2} - c_{d_3}) W_{21}^d W_{23}^{d*} \right] \\ & = \sqrt{\frac{m_b}{m_d}} (c_{d_1} - c_{d_3}) \frac{f_{d_1}}{f_{d_3}} \mathcal{O}(1), \end{aligned} \quad (46)$$

the last step simply using the fact that $(c_{d_1} - c_{d_3}) > (c_{d_2} - c_{d_3})$, so that at least the parametric dependence (up to order one corrections) is satisfied.

Finally we show the calculation for the coupling \tilde{a}_{12}^d , between down and strange quarks, which can be obtained with a slightly different choice of unitarity relations. We have

$$\begin{aligned} \tilde{a}_{12}^d = \sqrt{\frac{m_s}{m_d}} & \left[(c_{q_1} - c_{q_2}) U_{11}^{Q_d*} U_{12}^{Q_d} + (\mathcal{I}(c_{q_3}) - c_{q_2}) U_{31}^{Q_d*} U_{32}^{Q_d} \right. \\ & \left. + (\mathcal{I}(c_{q_4}) - c_{q_2}) U_{41}^{Q_d*} U_{42}^{Q_d} \right] + \mathcal{O}\left(\frac{m_d}{m_s}\right). \end{aligned} \quad (47)$$

Taking into account hierarchies in the wavefunctions f_i , we can directly neglect higher order terms and obtain

$$\tilde{a}_{12}^d = \sqrt{\frac{m_s}{m_d}} \left(c_{q_1} - c_{q_2} \right) \frac{f_{Q_1}}{f_{Q_2}} \mathcal{O}(1). \quad (48)$$

All other terms in the down and the up sector can be computed in the same manner, and thus one can derive from precise analytical expressions like those in Eqs. (42), (45) and (47), the much simpler approximative results presented in the main text in Eqs. (26), (27) and (31).

[1] L. Randall and R. Sundrum, Phys. Rev. Lett. **83**, 3370 (1999); L. Randall and R. Sundrum, Phys. Rev. Lett. **83**, 4690 (1999).

- [2] T. Gherghetta and A. Pomarol, Nucl. Phys. B **586**, 141 (2000); Y. Grossman and M. Neubert, Phys. Lett. B **474**, 361 (2000).
- [3] H. Davoudiasl, J. L. Hewett and T. G. Rizzo, Phys. Lett. B **473**, 43 (2000); A. Pomarol, Phys. Lett. B **486**, 153 (2000); S. Chang, J. Hisano, H. Nakano, N. Okada and M. Yamaguchi, Phys. Rev. D **62**, 084025 (2000).
- [4] K. Agashe, A. Delgado, M. J. May and R. Sundrum, JHEP **0308**, 050 (2003). K. Agashe and R. Contino, Nucl. Phys. B **742**, 59 (2006); K. Agashe, R. Contino, L. Da Rold and A. Pomarol, Phys. Lett. B **641**, 62 (2006); M. Carena, E. Ponton, J. Santiago and C. E. M. Wagner, Nucl. Phys. B **759**, 202 (2006) and Phys. Rev. D **76**, (2007) 035006; R. Contino, L. Da Rold and A. Pomarol, Phys. Rev. D **75**, 055014 (2007); A. D. Medina, N. R. Shah and C. E. M. Wagner, Phys. Rev. D **76**, 095010 (2007); C. Bouchart and G. Moreau, C. Bouchart, G. Moreau, Nucl. Phys. **B810**, 66-96 (2009).
- [5] S. J. Huber and Q. Shafi, Phys. Lett. B **498**, 256 (2001); C. Csaki, A. Falkowski and A. Weiler, JHEP **0809**, 008 (2008); M. Blanke, A. J. Buras, B. Duling, S. Gori and A. Weiler, JHEP **0903** (2009) 001.
- [6] W. D. Goldberger and M. B. Wise, Phys. Rev. Lett. **83**, 4922 (1999).
- [7] C. Csáki, M. L. Graesser and G. D. Kribs, Phys. Rev. D **63**, 065002 (2001).
- [8] G. F. Giudice, R. Rattazzi and J. D. Wells, Nucl. Phys. B **595**, 250 (2001).
- [9] S. Bae, P. Ko, H. S. Lee and J. Lee, Phys. Lett. B **487**, 299 (2000); K. M. Cheung, Phys. Rev. D **63**, 056007 (2001); J. L. Hewett and T. G. Rizzo, JHEP **0308**, 028 (2003); D. Dominici, B. Grzadkowski, J. F. Gunion and M. Toharia, Nucl. Phys. B **671**, 243 (2003); D. Dominici, B. Grzadkowski, J. F. Gunion and M. Toharia, Acta Phys. Polon. B **33**, 2507 (2002); J. F. Gunion, M. Toharia and J. D. Wells, Phys. Lett. B **585**, 295 (2004); M. Toharia, Phys. Rev. D **79**, 015009 (2009); K. Huitu, S. Khalil, A. Moursy, S. K. Rai, A. Sabanci, [arXiv:1105.3087 [hep-ph]].
- [10] C. Csaki, J. Hubisz and S. J. Lee, Phys. Rev. D **76**, 125015 (2007).
- [11] A. Azatov, M. Toharia and L. Zhu, Phys. Rev. D **80**, 031701 (2009).
- [12] K. Agashe, R. Contino, Phys. Rev. D **80**, 075016 (2009).
- [13] A. Azatov, M. Toharia and L. Zhu, Phys. Rev. D **80**, 035016 (2009).
- [14] T. Aaltonen *et al.* [CDF Collaboration], Phys. Rev. D **83**, 112003 (2011); T. Aaltonen *et al.* [CDF Collaboration], Phys. Rev. Lett. **101**, 202001 (2008); V. M. Abazov *et al.* [D0 Collaboration], Phys. Rev. Lett. **100** 142002 (2008).
- [15] E. Lunghi, A. Soni, Phys. Lett. **B697**, 323-328 (2011).
- [16] B. Holdom, Phys. Rev. D **54** (1996) 721; M. Maltoni, V. A. Novikov, L. B. Okun, A. N. Rozanov and M. I. Vysotsky, Phys. Lett. **B476** (2000) 107; H. J. F. He, N. Polonsky and S.

- f. Su, Phys. Rev. **D64** (2001) 053004; V. A. Novikov, L. B. Okun, A. N. Rozanov and M. I. Vysotsky, Phys. Lett. **B529** 111 (2002); G. D. Kribs, T. Plehn, M. Spannowsky and T. M. P. Tait, Phys. Rev. **D76** 075016 (2007).
- [17] M. Frank, B. Korutlu, M. Toharia, Phys. Rev. D **84**, 075009 (2011).
 - [18] C. Charmousis, R. Gregory, V. A. Rubakov, Phys. Rev. **D84**, 075009 (2011).
 - [19] ATLAS Collaboration, <https://twiki.cern.ch/twiki/bin/view/AtlasPublic/AtlasResultsEPS2011>.
 - [20] CMS Collaboration, CMS PAS HIG-11-011, <http://cms.web.cern.ch/cms/News/2011/EPS2011>.
 - [21] C. Charmousis, R. Gregory, V. A. Rubakov, Phys. Rev. **D62**, 067505 (2000).
 - [22] S. Casagrande, F. Goertz, U. Haisch, M. Neubert and T. Pfoh, JHEP **0810**, 094 (2008).
 - [23] G. Burdman and L. Da Rold, JHEP **0712**, 086 (2007); G. Burdman, L. Da Rold, R. D'E. Matheus, Phys. Rev. **D82**, 055015 (2010).
 - [24] W. Buchmuller and D. Wyler, Nucl. Phys. B **268**, 621 (1986).
 - [25] F. del Aguila, M. Perez-Victoria and J. Santiago, Phys. Lett. B **492**, 98 (2000); JHEP **0009**, 011 (2000).
 - [26] A. J. Buras, [hep-ph/9806471].
 - [27] M. Bona *et. al.* [UTfit Collaboration], JHEP **03**, 049 (2008).
 - [28] R. Barate *et. al* (LEP working group for Higgs boson searches, ALEPH Collaboration, DELPHI Collaboration, L3Collaboration and OPAL Collaboration), Phys. Lett. B **565**, 61 (2003).
 - [29] D. Benjamin *et al.*, [CDF and D0 Collaborations] arXiv:1108.3331 [hep-ex].
 - [30] The ATLAS Collaboration, ATL-CONF-2011-135, presented at 25th International Symposium on Lepton Photon Interactions at High Energies, Mumbai, India, 22-27 Aug 2011, to appear in the proceedings.
 - [31] W. D. Goldberger, B. Grinstein, W. Skiba, Phys. Rev. Lett. **100**, 111802 (2008).
 - [32] H. Davoudiasl, E. Ponton, Phys. Lett. **B680**, 247 (2009).